

Article

Modelling, Simulation and Performance Validation of the Pneumatic Actuation System of a Rehabilitation Device of the Human Hand Joints

Ovidiu Filip, Andrea Deaconescu  and Tudor Deaconescu * 

Department of Industrial Engineering and Management, Transilvania University of Brasov,
500036 Braşov, Romania

* Correspondence: tdeacon@unitbv.ro; Tel.: +40-745-757850

Abstract: The passive mobilization of the hand joints by means of dedicated equipment accelerates patient recovery and decreases significantly the costs of therapy. For this reason, research and development of such equipment is essential. Important reductions in the development cycle duration of such equipment can be achieved by means of a specific technique known as Model-Based Design. Starting from these considerations, this paper puts forward a Model-Based Design approach to the study of a new concept of rehabilitation equipment of the hand joints actuated by a pneumatic muscle. The originality of the paper consists in the MATLAB-based rendering of the functional model of the rehabilitation equipment actuation system and in the presented simulation results. The purpose of this research was to obtain information concerning the behavior of the proposed system and to predict its performance prior to it being built physically. After simulation, the results are compared to the operational performance of the experimental model. The conclusion shows that the proposed operational model describes accurately the actual behavior of the system and can be used for future optimization of the rehabilitation equipment.



Citation: Filip, O.; Deaconescu, A.; Deaconescu, T. Modelling, Simulation and Performance Validation of the Pneumatic Actuation System of a Rehabilitation Device of the Human Hand Joints. *Appl. Sci.* **2023**, *13*, 1649. <https://doi.org/10.3390/app13031649>

Academic Editors: Carlos A. Jara and Juan Antonio Corrales Ramón

Received: 21 December 2022

Revised: 22 January 2023

Accepted: 23 January 2023

Published: 28 January 2023



Copyright: © 2023 by the authors. Licensee MDPI, Basel, Switzerland. This article is an open access article distributed under the terms and conditions of the Creative Commons Attribution (CC BY) license (<https://creativecommons.org/licenses/by/4.0/>).

Keywords: Model-Based Design; simulation; wrist rehabilitation equipment; pneumatic muscle

1. Introduction

Lesions of the upper limbs while frequently painful can cause lasting sequelae that have nevertheless a high recovery potential, hence the high odds of patients swiftly resuming everyday activity and work. The new and efficient therapy methods available to-date led to reduced recovery periods of patients suffering from such trauma and to a smaller failure rate of the treatment of such pathologies [1]. In addition, patient recovery can be accelerated by using innovative recovery equipment of the upper limbs.

The complex structure of the hand renders it perfectly adapted to human activities, such as the gripping and holding of objects, non-verbal communication by gestures, expression of fondness, etc. The role of the rest of the upper limb segments (shoulder, arm, elbow, forearm) is to ensure a favorable positioning of the hand to carry out these functions. The skeleton of the palm and fingers includes 27 bones and due to its complexity is prone to traumatic lesions that can partially or totally inhibit the hand's functions. The wrist is a multi-articular structure that allows flexion, extension, circumduction, radial and ulnar deviation.

The majority of the hand joints' affections are of the traumatic lesion type, the treatment of which starts with immobilization in a cast. Prolonged immobilization of the hand joints leads, however, to muscular hypertrophy and bone demineralization. Thus, a swift transition to motion-based recovery becomes an imperative.

After approximately three days of immobilization, the use of customized orthoses is recommended, also light physical exercise and active and passive mobilization of the fingers [2]. This recovery stage is followed by continuous passive motion (CPM), namely the

mechanized exercising of the affected joint without involving effort made by the patient's muscles. Continuous passive motions are aimed at preventing the building up of fibrous tissue and reducing joint stiffness. All these procedures are applied in order to improve muscle tonus and the sensitive, psychological and social as well as occupational status.

Passive mobilization of the hand joints can be done manually by a physical therapist, or, as is frequently the case, mechanically by means of dedicated rehabilitation equipment. Such equipment can be set to ensure optimum motion parameters such as the rotation amplitude and displacement velocity of the joints, as well as the duration and frequency of the recovery exercising. The magnitude of the applied forces is also controllable so that the rehabilitation exercises do not cause additional patient suffering.

Most of the CPM-based rehabilitation equipment for the hand joints is driven electrically, the most representative of these being described further on. The Kinetec Maestra Hand and Wrist Tabletop CPM allows following hand and/or wrist surgery up to nine different exercises for the rehabilitation of the fingers, thumb and wrist [3]. The motion limits possibly attainable for the fingers are 45° hyperextension and 270° flexion, and for the wrist, 90° extension and 55° flexion.

Another equipment is the Kinetec—8091 Portable Hand CPM designed for rehabilitation following the prosthetic replacement of the finger joints. Range of motion, speed, pause times and force can be set and displayed by a remote digital hand control [4]. The MIT-MANUS system developed at the Massachusetts Institute of Technology has the following motion limits: flexion/extension 60°/60°, abduction/adduction 30°/45° and pronation/supination 70°/70° [5]. Another continuous passive motion equipment is the QAL Medical W2 Wrist CPM designed for CPM-based rehabilitation of a wrist joint in flexion/extension and ulnar/radial deviation, or a combination of both. The motion limits of the wrist here are of 0°–90° for flexion/extension, and up to 90° for ulnar/radial deviation [6]. The 6000 Hand CPM OrthoAgility® is another example of electrically actuated equipment that is used for post-fracture recovery, reconstructive surgery on bone, cartilage, tendons and ligaments, and allows patients to achieve a full composite fist of 270° [7]. The WaveFlex Hand system developed by Remington Medical is a light construction deployable both in hospital and in patients' homes. It supports the performing of rehabilitation exercises within the limits of hand joint biomechanics [8].

In addition to the enumerated characteristics, the electrically actuated devices exemplified above also have a compliant behavior, that is, they adapt to a possible resistance put up by the patient upon the onset of pain. It is known that during rehabilitation exercising, certain limits of the motions can be exceeded; beyond that the patient may feel pain. The response time of the rehabilitation equipment from the sensing of pain to the execution of corrections, that is, until compliance is activated, should be as short as possible, this being an important feature of a recovery device. Ensuring the compliance of electrically driven rehabilitation devices, that is, the swift adaptation of the system to the concrete situation determined by the patient state, entails, however, excessive sensorization and the implementation of complicated control diagrams, all of these leading eventually to cost-intensive equipment of the order of thousands of euros [9].

Under these circumstances, it becomes a requirement to identify new solutions for reasonably costed rehabilitation equipment adapted to the budgets of health services or those of patients. A solution is the elimination of most sensors, thus simplifying the control diagrams and implicitly reducing costs. This can be achieved by introducing adjustable compliance actuators, known as ACAs, such as pneumatic muscles that due to the compressibility of air have an inherently compliant behavior. Pneumatic muscles ensure safe interaction with human operators also by their ability of storing and releasing energy into passive elastic elements [10].

Deploying pneumatic actuation in medical rehabilitation equipment is not widespread. Hesitation in using pneumatic drives is due to the requirement of air preparation systems, noisy operation or the impossibility of high accuracy positioning of the mobile elements. Notwithstanding, pneumatic actuation offers advantages such as the possibility of de-

veloping “pneumatic springs” for end-of-stroke damping, all being determined by air compressibility. Another favorable feature is compliance, the inverse of rigidity, which allows deviations from a certain position of equilibrium in case external forces act upon the system.

To date, only few medical rehabilitation devices actuated by pneumatic muscles are known, most being patents and/or prototypes. An example of pneumatic muscle actuated rehabilitation equipment already available on the market for an affordable couple of hundred euros is the Hand Mentor Pro, developed for exercising the hand in view of the recovery of its gripping ability [11].

EXOWRIST (a prototype for wrist rehabilitation) is another example of rehabilitation equipment deploying four pneumatic muscles as actuators and ensuring two degrees of mobility. The advantages of this device are its low price and high portability for autonomous and independent use [12].

Another wrist rehabilitation system with a single degree of mobility is in its prototype phase, proposed by Meng et.al. [13]. The equipment uses two pneumatic muscles in antagonist operation mode, causing the hand support to conduct flexion and extension motions.

The review and analysis of the state of art of upper limb medical rehabilitation equipment constructions yielded certain conclusions regarding the requirements that these systems have to meet. Concretely, both portability and the compliant behavior of the equipment must be ensured at the lowest possible cost. Each of the known electrical or pneumatic equipment meets part of these requirements. Starting from these facts, this paper analyzes a novel recovery system able to mobilize simultaneously both wrist and finger joints and fulfil the requirements detailed above.

A single pneumatic muscle was used for mobilizing the joints, and the support for the palm and fingers was an innovative construction based on the Fin-Ray effect. This paper is focused on the modelling and simulation of the rehabilitation equipment actuation system using the specific techniques of Model-Based Design, and subsequently the performance of the simulated model is compared to the operational performance of the experimental model. The simulation results offer valuable information on the forces/torques occurring in patient–equipment interaction, information to be used for the improvement and optimization of the system’s mechanical construction.

The structure of the paper includes a second section that defines the motion parameters to be met by the new equipment as well as a number of aspects regarding the construction of its actuation system. Further on, the third section of the paper presents the concept of Model-Based Design (MBD) that underlies the modelling and simulation of the rehabilitation equipment’s actuation system. MATLAB® is proposed as the specific MBD work tool. After presenting the operational model of the studied system and its characteristic diagrams, the fourth section features the experimental results obtained by testing the physical model and carries out a comparison with those predicted by simulation. The last chapter is dedicated to the conclusions of the study.

2. Requirements of the Novel Rehabilitation Equipment and Constructive Principle

Developing a rehabilitation equipment for the hand joints starts from the information derived from studying the biomechanics of the upper limb. Devising a partial articular assessment consisting of establishing the maximum rotations of the joints in the sagittal plane of reference reveals the essential motions that should be achieved by means of a rehabilitation device. Thus, it followed that the motions that have to be conducted are the flexion and extension of the radiocarpal, metacarpophalangeal and interphalangeal joints (Figure 1).

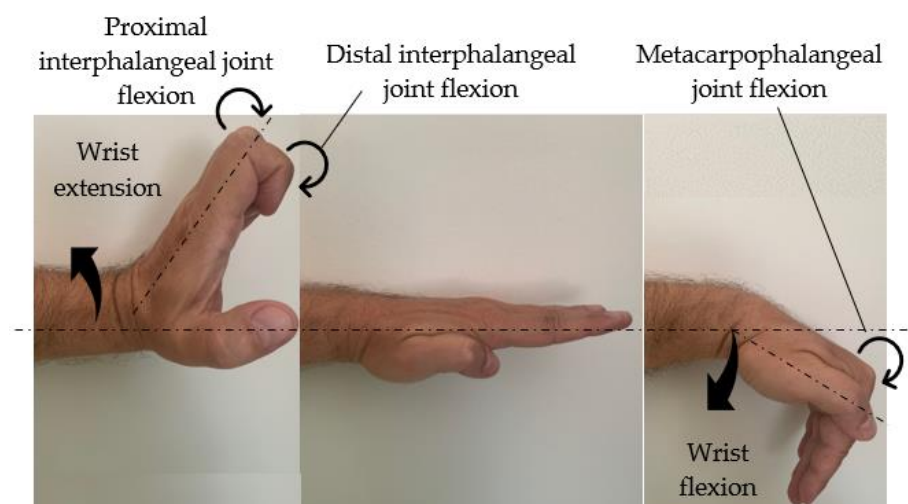


Figure 1. Flexion/extension of the wrist and flexion of the joints of the fingers.

The natural mobility limits of these joints were taken from literature and are shown in Table 1 together with the maximum rotational speeds that have to be provided by the actuation systems of the rehabilitation equipment [7].

Table 1. Mobility characteristics of the wrist and finger joints.

Joint	Motion	Rotation Angle [°]	Rotational Speed [°/min]
Wrist	Flexion	0 to 80	30 to 180
	Extension	0 to 70	
Joints of the fingers	Metacarpophalangeal Flexion	0 to 90	55 to 440
	Metacarpophalangeal Extension	0 to 90	
	Proximal Flexion	0 to 120	
	Proximal Extension	0 to 90	
	Distal Flexion	0 to 90	
	Distal Extension	0 to 90	

Based on these data, the authors and their team developed a rehabilitation equipment for the wrist and finger joints (Figure 2), the comprehensive constructive description and performance of which are presented in [12].

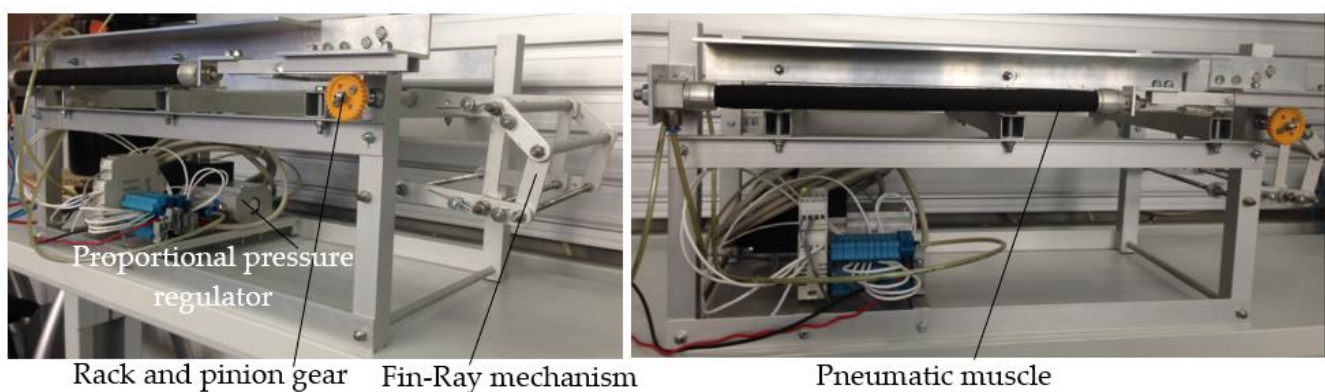


Figure 2. Construction of the rehabilitation equipment.

The innovative character of this equipment resides in the bioinspired conception of the palm support based on the Fin-Ray effect specific to the fins of the manta ray. The structure of this device consists of two series-connected bar mechanisms mounted in a V-shape pyramid structure. Upon setting joint A into rotation, the entire construction is deformed as shown in the schematics of Figure 3 [14].

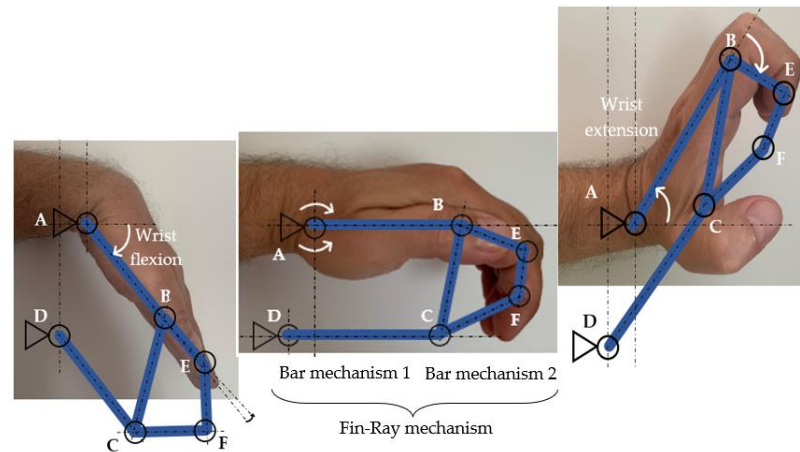


Figure 3. Motions of the hand support.

An important feature of this constructive solution is that the rehabilitation equipment allows the simultaneous generation of the flexion and extension of the radiocarpal, metacarpophalangeal and interphalangeal joints.

Joint A is rotated by means of a rack and pinion mechanism that uses a pneumatic muscle as the motor. By feeding air at different pressures to the pneumatic muscle, the rack is displaced in both directions, the magnitude of the respective strokes being controlled. Figure 4 shows the actuation system of joint A.



Figure 4. Actuation system of joint A.

The pneumatic muscle used for the actuation of the equipment, manufactured by the German company Festo, has a 10 mm interior diameter, the length of the active part being of 300 mm and the maximum achievable stroke of 60 mm [15]. The pinion has 30 clogs and a module of 1 mm. Starting from the data in Table 1 (the maximum flexion of the wrist is of 80° and its maximum extension is 70°), the necessary axial contraction of the muscle (and implicitly the stroke of the rack) should be of 39.25 mm.

Further on, the results obtained by simulation and by testing the operation of the actuation system of the novel hand joint rehabilitation equipment will be presented comparatively.

3. Modelling and Simulation of the Actuation System of the Rehabilitation Device

3.1. Model-Based Design (MBD)

Model-Based Design (MBD) techniques are used for understanding the operational behavior of a physical system in project phase by systematically using models throughout the entire process. In order to design, analyze and validate dynamic systems, MBD uses a model/mathematical algorithm and its graphic/visual representation. MBD facilitates

identifying design errors from the very initiation of the development process, thus saving time and improving the quality of the analyzed system.

Modelling and simulation of the actuation system of the rehabilitation equipment requires using physical and/or logical representations in order to generate data and to support decision making or to devise predictions related to the system [16]. The model is a representation of a system or process, while a simulation model is a representation that includes time and the changes occurring in time [17].

In general, simulation does not yield optimal values as is the case with analytical modelling, but merely information that describes the phenomenon by experimenting, called descriptors. Simulation can be used to predict the behavior or performance of systems under certain simplified testing conditions [18].

Further on, a simulation model of the new rehabilitation equipment will be presented, devised by MATLAB® numerical calculation medium.

3.2. Modelling and Simulation with MATLAB-Simulink

The modelling and simulation of dynamic systems by means of MATLAB® are specific Model-Based Design techniques that can reduce the duration of the product development cycle by up to 50% [19]. For the modelling and simulation of systems, MATLAB® includes a graphic extension called Simulink® by means of which systems can be modelled with the help of block type elements grouped into categories, such as transfer functions, summing junctions, etc. as well as function generators and oscilloscopes [20]. The Simulink® approach is based on a time-based and multi-rate system.

On its turn, Simulink® includes Simscape™, a graphical programming environment for modelling, simulating and analysis of dynamic systems. Simscape™ Fluids™ is used for the modelling and simulation fluid systems that provide a set of components specific for this field.

The modelling and simulation of the actuation system of the hand joints rehabilitation equipment by means of MATLAB® R2021b–Simulink®–Simscape™ Fluids™ starts with establishing beforehand a recovery exercise based on a sequence of motions recommended by the physical therapist. Figure 5 presents and illustrates such an exercise that further serves as the basis for conceiving the MATLAB® functional model consisting of blocks (Figure 6). The duration of the exercise is of 60 s. The first half of the cycle is designed to generate extension, more accelerated in the beginning and slower as the upper limit of this motion is approached ($+70^\circ$) when the onset of pain is possible. Flexion is conducted during the time interval of $t \in [30, 60]$ seconds, the last part of this motion being also slowed down for the same reasons.

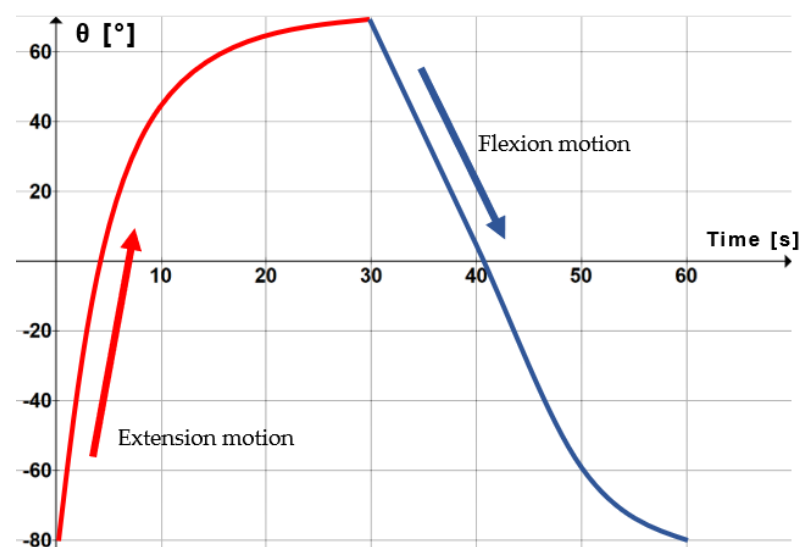


Figure 5. Sequence of recovery motions to be generated by the equipment.

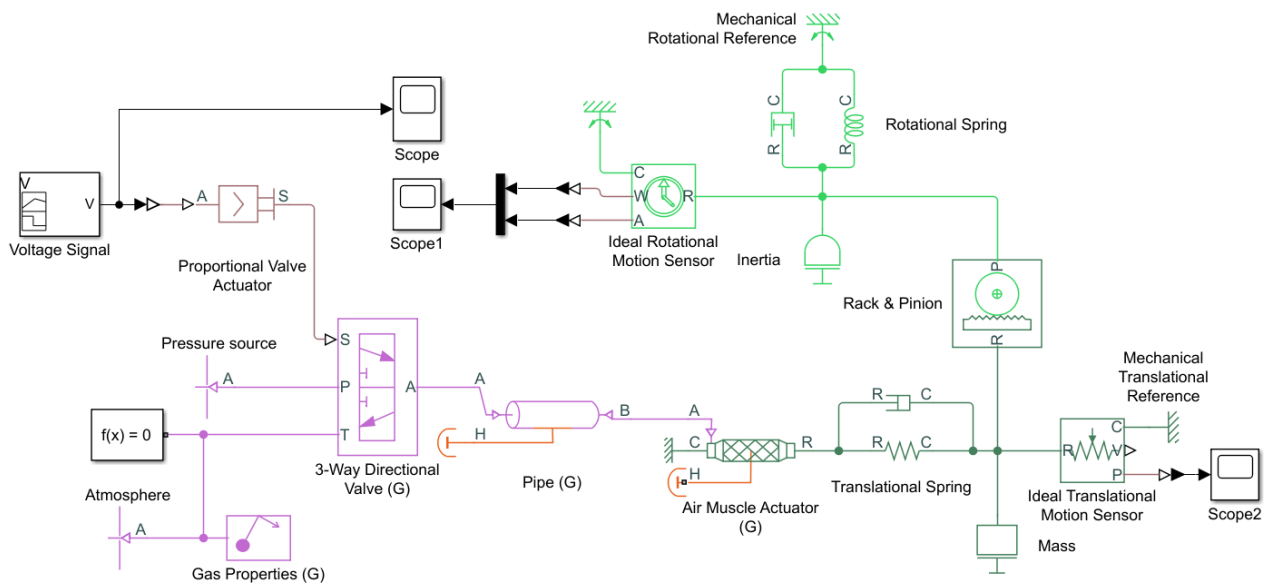


Figure 6. Functional model of the rehabilitation equipment actuation system.

The central block of the model is that of the pneumatic muscle (Air Muscle Actuator), its characteristics and analysis pattern being based on the Chou and Hannaford model [21]. Port A is the gas conserving port associated with the actuator inlet. Port H is the thermal conserving port associated with the temperature of the gas inside the actuator. Ports R and C are the mechanical translational conserving ports associated with the two end caps of the actuator. The main dimensional characteristics of the pneumatic muscle were introduced as input parameters of the block.

The pneumatic muscle is fed air from the Pressure source block, wherefrom the gas passes to a 3-Way Directional Valve. Ports P, T and A are associated with feeding, airing and the connection to the equipment's actuator, respectively. The valve opening fraction between -1 and 1 is set by the physical signal port S. Port S receives a voltage signal by means of a Proportional Valve Actuator. A complete rehabilitation cycle of the wrist (an extension and a flexion) conducted in 60 s was simulated imposing a signal of the form shown in Figure 7 as the input of the Proportional Valve Actuator. The Proportional Valve Actuator converts the control input into the valve actuator position, the signal sent to the 3-Way Directional Valve having the form shown in Figure 8.

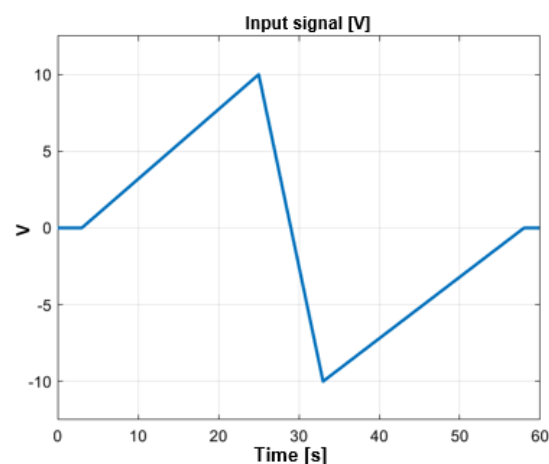


Figure 7. Characteristics of the signal provided by the signal generator (Voltage Signal).

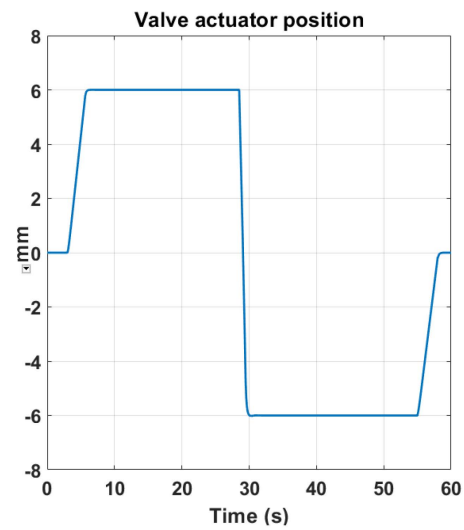


Figure 8. Variation versus time of the output signal of the Proportional Valve Actuator.

During a cycle of rehabilitation exercising (60 s), the feed pressure of the pneumatic muscle and its axial contraction vary according to the graphs in Figures 9 and 10.

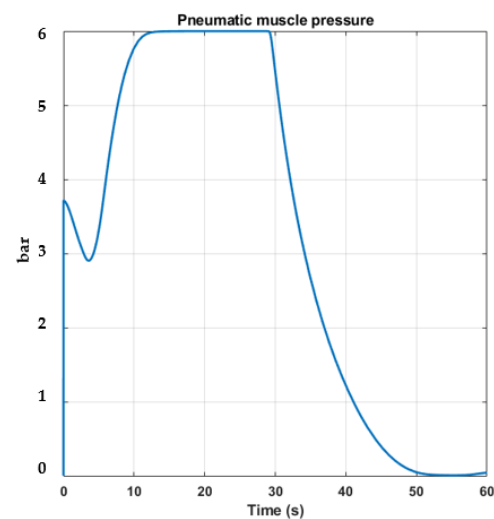


Figure 9. Variation versus time of the pneumatic muscle feed pressure.

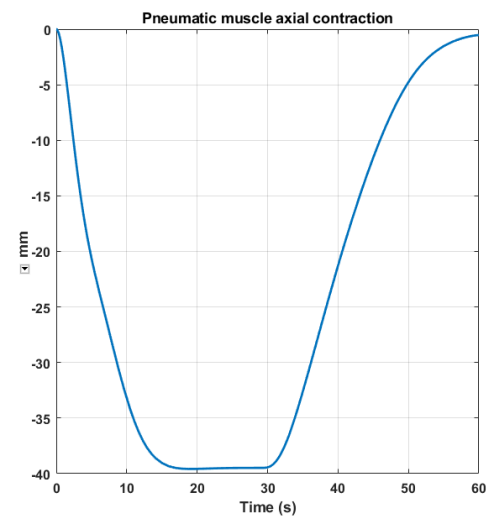


Figure 10. Variation versus time of the pneumatic muscle axial contraction.

The graphs shown in the figures above were generated by an Ideal Translational Motion Sensor block. This block measures velocity and/or displacement of the free end of the pneumatic muscle. Figure 10 shows a maximum stroke carried out by the rack of the mechanism (the free end of the pneumatic muscle) of 39.486 mm. This value is sufficient to obtain a rotation of the lever AB in an interval ranging from -80° to $+71.2387^\circ$ (Figure 11).

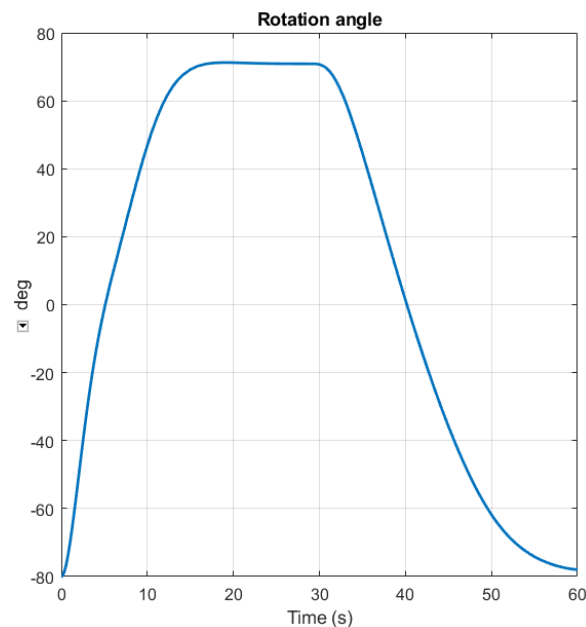


Figure 11. Variation versus time of the rotation angle of lever AB.

Figure 12 shows the evolution of the angular velocity of lever AB of the Fin-Ray mechanism over the duration of a rehabilitation cycle:

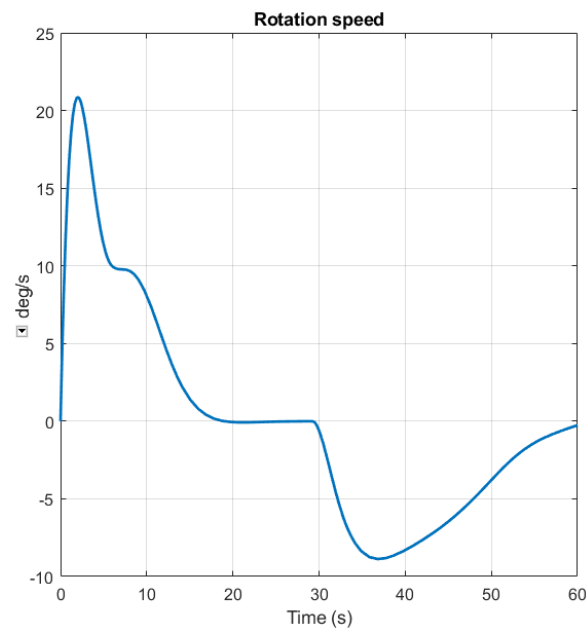


Figure 12. Variation versus time of the angular velocity of lever AB.

Figures 11 and 12 were obtained by means of the Ideal Rotational Motion Sensor block that measures the angular velocity and/or rotation angle of the rotating components of the equipment. The Scope blocks attached to the sensors display the signals generated during simulation.

The simulation by means of MATLAB® of the actuation system's behavior confirmed the form of the motion curves established by the physical therapist (Figure 5) as well as the targeted limits of the motions. The motion limits and the operational behavior of the rehabilitation equipment determined by simulation will be further on validated by testing.

4. Testing and Validation

The experimental results concerning the performance of the equipment were presented in detail in [14]. Of interest for the present study is to identify dependencies of form $p = p(t)$ and $\theta = \theta(t)$ that meet the specifics of a rehabilitation exercise such as the one proposed in Figure 5 (p = air pressure; θ = wrist rotation angle). Further on, the sequence of the steps of such a rehabilitation exercise is presented.

At rest, in the absence of compressed air, the pneumatic muscle is relaxed, and the rack is displaced maximum to the right (Figure 4). The position of the rehabilitation mechanism in this case corresponds to a maximum flexion of the wrist (lever AB turned to -80°).

In order to initiate a rehabilitation exercise, the first step is to set the palm support to zero position with a horizontal lever AB. This motion is meant to allow fixing the patient's hand on the palm support. For this, the pneumatic muscle is charged with air to a pressure at which it is caused to shorten and consequently to generate a sufficient displacement of the rack so that lever AB turns by 80° . Experimentally, it was determined that charging the pneumatic muscle with air at a pressure of 2.72 bar will shorten and displace the rack by 19.62 mm, and consequently lever AB will reach its horizontal position (Figure 13a).

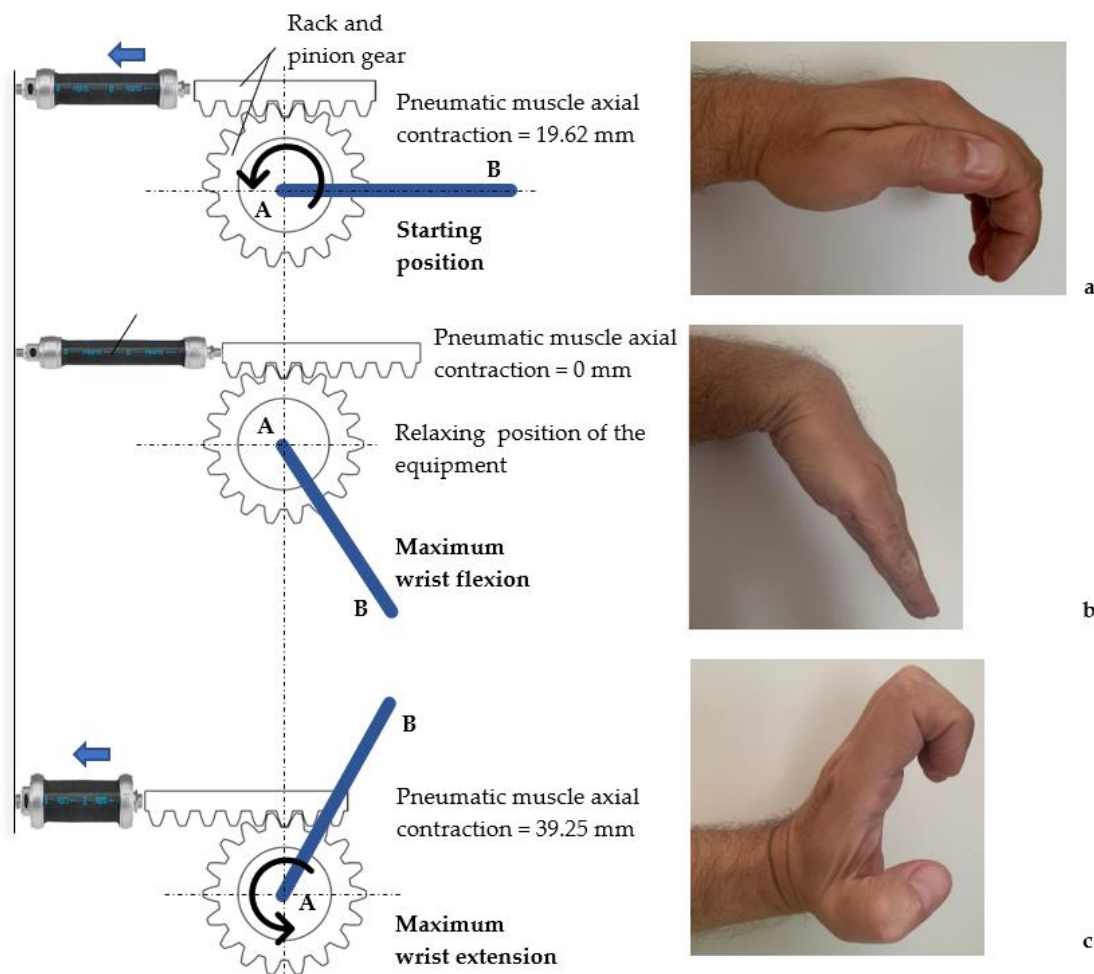


Figure 13. Positions of lever AB while the pneumatic muscle is charged with air: (a) Starting position; (b) Maximum wrist flexion; (c) Maximum wrist extension.

Decreasing the air pressure in the muscle to 0 bar causes the flexion of the wrist (Figure 13b), while increasing the pressure leads to extension (Figure 13c).

Compressed air is fed to the muscle through a proportional pressure regulator controlled by a reference module, produced by Festo AG & Co Esslingen, Germany (Figure 14). The continuous modification of the pressure fed to the proportional pressure regulator causes the permanent variation in time of the air pressure in the pneumatic muscle and allows for modifying the compliance of the entire system. This is a pressure-based control scheme where the pressure within the pneumatic muscle is measured and controlled in a closed loop.

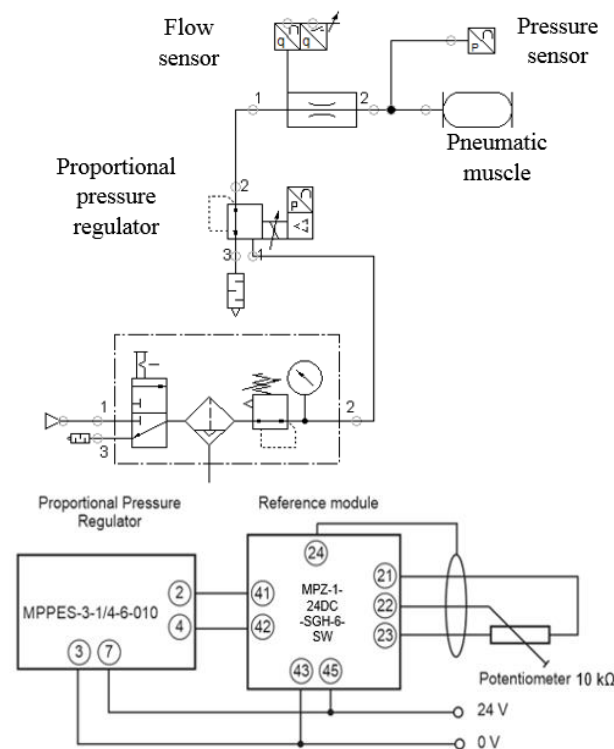


Figure 14. Control of the rehabilitation equipment by means of a proportional pressure regulator.

Figure 15 shows the experimentally determined variation curves of the feed pressure versus time. The variation in time of the pneumatic muscle feed pressure was controlled so that the form of the resulting curves is as close as possible to that obtained consequently via modelling and simulation by means of MATLAB® (Figure 9).

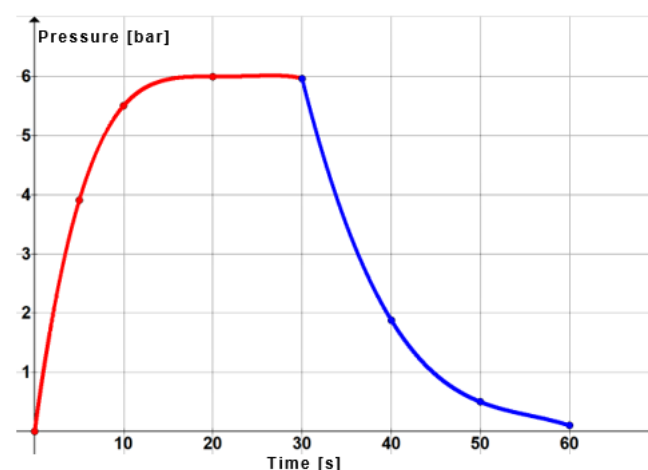


Figure 15. Charging/discharging curves of the pneumatic muscle with air during a rehabilitation exercise cycle.

Equations (1) and (2) represent the functions that describe the variation of pressure at the charging of the pneumatic muscle (for conducting extension) and at the discharging of air (for conducting flexion), respectively:

$$p(t) = -2.59 \cdot 10^{-5} \cdot t^4 + 0.0023 \cdot t^3 - 0.076 \cdot t^2 + 1.1058 \cdot t \quad t \in [0, 30) \quad (1)$$

$$p(t) = -0.0003 \cdot t^3 + 0.0479 \cdot t^2 - 2.7003 \cdot t + 51.6 \quad t \in [30, 60] \quad (2)$$

Knowing these functions is necessary for controlling the proportional pressure regulator. A specially developed computer program based on the above polynomial equations is loaded to a PLC. The PLC sends an electric signal to the proportional pressure regulator whose voltage is continuously modified according to the polynomial function.

The charging/discharging of the pneumatic muscle with pressure according to the curves in Figure 15 allowed the determining of the variation versus time of the muscle's axial contraction (Δl). This quantity was measured by a linear potentiometer provided by German company Festo and which has the following characteristics: measured stroke: 200 mm; electrical resistance: $10 \text{ k}\Omega \pm 20\%$; supply voltage: 13–30 V DC; output voltage: 0–10 V DC.

Table 2 presents the measured sets of values ($t, \Delta l$) and Figure 16 shows the curves that describe the variation of the axial contraction in time.

Table 2. Variation in time of the pneumatic muscle axial contraction.

t [s]	0	10	20	30	40	50	60
Δl [mm]	0	−30.5	−38.1	−38.2	−22.1	−8.1	−1.2

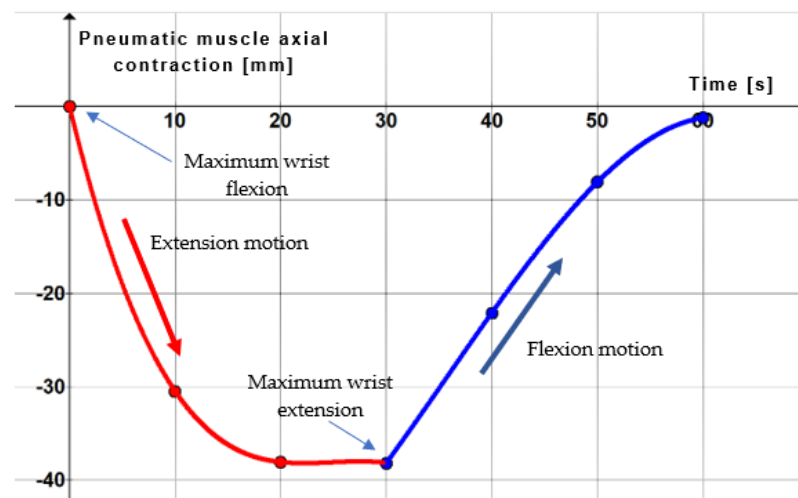


Figure 16. Variation versus time of the pneumatic muscle axial contraction.

The dots represent the measured values of the axial contractions, and the continuous lines show the polynomial regression curves suggested by Graph v. 4.4.2 software.

The dependencies of $\Delta l = f(t)$ type proposed by Graph software for the two curves represented above are:

$$\Delta l(t) = -0.00256 \cdot t^3 + 0.1915 \cdot t^2 - 4.7083 \cdot t \quad t \in [0, 30) \quad (3)$$

$$\Delta l(t) = -0.00083 \cdot t^3 + 0.0895 \cdot t^2 - 1.5716 \cdot t - 49.1 \quad t \in [30, 60] \quad (4)$$

The variation in time of the rotation angle of lever AB, respectively of the wrist, was measured by means of a E6A2-CS5C Omron rotary encoder mounted on the axis of joint A. Table 3 presents the measured values, while the corresponding curves are shown

in Figure 17. The dots represent the measured values of the angles, being connected by polynomial regression curves proposed by Graph software.

Table 3. Variation in time of the wrist rotation angle.

t [s]	0	10	20	30	40	50	60
θ [°]	−80	44.5	67.1	67.3	0	−62.7	−77.9

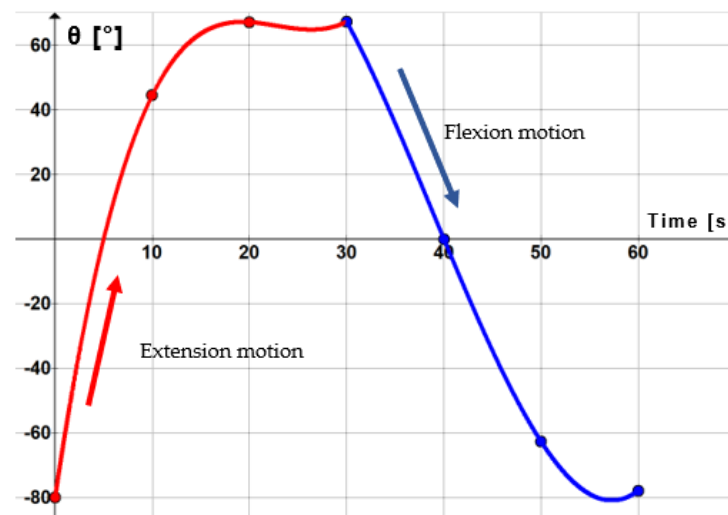


Figure 17. Variation versus time of the wrist rotation angle.

The estimating functions of the variation in time of the wrist rotation angle proposed by Graph are the following:

$$\theta(t) = 0.0133 \cdot t^3 - 0.907 \cdot t^2 + 20.195 \cdot t - 80 \quad t \in [0, 30) \quad (5)$$

$$\theta(t) = 0.0072 \cdot t^3 - 0.835 \cdot t^2 + 25.265 \cdot t - 132.2 \quad t \in [30, 60] \quad (6)$$

The obtained experimental results materialized in the curves of Figures 16 and 17 confirm the validity of the proposed functional model generated and simulated by means of MATLAB®. This is proved by the two graphs being very close as to their form and values to the modelled and simulated ones represented in Figures 10 and 11, the differences being minimal.

5. Conclusions

By using Model-Based Design (MBD) techniques, this paper presents a simulation model of the actuation system of an innovative hand joints rehabilitation device conceived by the authors based on the Fin-Ray effect. This model was devised by means of numerical calculation software MATLAB® and its components Simulink®/Simscape™/Fluids™. The purpose of modelling and simulation was to obtain ante-factum information regarding the behavior of the proposed system and to predict its performance prior to its actual physical materialization.

The physical model was constructed after completed simulations conducted on the MATLAB® model that yielded a behavior of the rehabilitation device's actuation system that meets the imposed requirements. On the physical model, the real performance of the actuation system was measured followed by a comparison of the simulated and the measured values. The ensuing conclusion is that the results obtained by the two working methods are significantly close, which validates the functional model developed in MATLAB®. Consequently, this model lends itself with high confidence for future use in the optimization process of the proposed rehabilitation equipment.

Author Contributions: Conceptualization, O.F. and T.D.; methodology, T.D.; validation, O.F. and A.D.; writing—original draft preparation, A.D.; writing—review and editing, T.D.; supervision, T.D. All authors have read and agreed to the published version of the manuscript.

Funding: This research received no external funding.

Institutional Review Board Statement: Not applicable.

Informed Consent Statement: Not applicable.

Data Availability Statement: Not applicable.

Conflicts of Interest: The authors declare no conflict of interest.

References

1. Bulbul, M.K. Studiu Privind Incidenta Sindromului de Tunel Carpian, Complicație Tardivă a Fracturilor Metafizo-Epifizare Distale Ale Antebrațului, în Corelație Cu Tratamentul Acestora. Ph.D. Thesis, Oradea University, Oradea, Romania, 2015.
2. Skirven, T.M.; Osterman, A.; Fedorczyk, J.; Amadio, P.; Felder, S.; Shin, E. *Rehabilitation of the Hand and Upper Extremity*, 7th ed.; Elsevier: Philadelphia, PA, USA, 2020; Volume 1.
3. Kinetec Maestra Hand & Wrist Tabletop CPM. Available online: <https://www.medcomgroup.com/kinetec-maestra-hand-wrist-tabletop-cpm/> (accessed on 23 August 2022).
4. Kinetec—8091 Portable Hand CPM. Available online: <https://www.medcomgroup.com/content/Kinetec%208091%20Portable%20Hand%20CPM%20Operations%20Manual.pdf> (accessed on 23 August 2022).
5. Krebs, H.I.; Volpe, B.T.; Williams, D.; Celestino, J.; Charles, S.K.; Lynch, D.; Hogan, N. Robot-Aided Neurorehabilitation: A Robot for Wrist Rehabilitation. *IEEE Trans. Neural. Syst. Rehabil. Eng.* **2007**, *15*, 327–335. [CrossRef] [PubMed]
6. QAL Medical W2 Wrist CPM. Available online: <https://www.medcomgroup.com/qal-medical-w2-wrist-cpm/> (accessed on 23 August 2022).
7. OrthoAgility 6000 Hand CPM Specification Brochure. Available online: <https://pdf.medicalexpo.com/pdf/qal-medical/orthoagility-6000-hand-cpm-specification-brochure/93399-189906.html#open> (accessed on 30 August 2020).
8. Waveflex CPM. Available online: <https://www.remingtonmedical.com/product/waveflex-cpm/> (accessed on 30 August 2020).
9. Petre, I.; Deaconescu, A.; Sârbu, F.; Deaconescu, T. Pneumatic Muscle Actuated Wrist Rehabilitation Equipment Based on the Fin Ray Principle. *Stroj. Vestn.—J. Mech. Eng.* **2018**, *64*, 383–392.
10. Van Ham, R.; Sugar, T.G.; Vanderborght, B.; Hollander, K.W.; Lefeber, D. Compliant Actuator Designs. *IEEE Robot. Autom. Mag.* **2009**, *16*, 81–94.
11. The Hand Mentor Pro™. Available online: <http://stage.motusnova.com/products/hand-mentor-pro/> (accessed on 31 August 2020).
12. Andrikopoulos, G.; Nikolakopoulos, G.; Manesis, S. Motion Control of a Novel Robotic Wrist Exoskeleton via Pneumatic Muscle Actuators. In Proceedings of the 20th IEEE International Conference on Emerging Technologies and Factory Automation (ETFA), Luxembourg, 8–11 September 2015. [CrossRef]
13. Meng, W.; Sheng, B.; Klingner, M.; Liu, Q.; Zhou, Z.; Xie, S.Q. Design and control of a robotic wrist orthosis for joint rehabilitation. In Proceedings of the IEEE ASME International Conference on Advanced Intelligent Mechatronics, Busan, Republic of Korea, 7–11 July 2015; pp. 1235–1240.
14. Filip, O.; Deaconescu, A.; Deaconescu, T. Mechanical Design of a Bioinspired Compliant Robotic Wrist Rehabilitation Equipment. *Appl. Sci.* **2021**, *11*, 1246. [CrossRef]
15. Festo Fluidic Muscle DMSP/MAS. Available online: https://www.festo.com/rep/en_corp/assets/pdf/info_501_en.pdf (accessed on 28 August 2022).
16. Modeling and Simulation. Wikipedia. Available online: https://en.wikipedia.org/wiki/Modeling_and_simulation (accessed on 28 August 2022).
17. Carson, J.S., II. Introduction to modeling and simulation. In Proceedings of the 2005 Winter Simulation Conference, Orlando, FL, USA, 4 December 2005.
18. Marin, C.; Vasile, G. *Modeling and Simulation Techniques in Mechanical Engineering (Tehnici de Modelare si Simulare in Ingineria Mecanică)*; Bibliotheca: Târgoviște, Romania, 2011. (In Romanian)
19. Simulink. MathWorks. Available online: <https://www.mathworks.com/products/simulink.html> (accessed on 29 August 2022).
20. Simulink Basics Tutorial. Available online: https://ctms.engin.umich.edu/CTMS/index.php?aux=Basics_Simulink (accessed on 29 August 2022).
21. Chou, C.P.; Hannaford, B. Measurement and modeling of McKibben Pneumatic Artificial Muscles. *IEEE Trans. Robot. Autom.* **1996**, *12*, 90–102. [CrossRef]

Disclaimer/Publisher's Note: The statements, opinions and data contained in all publications are solely those of the individual author(s) and contributor(s) and not of MDPI and/or the editor(s). MDPI and/or the editor(s) disclaim responsibility for any injury to people or property resulting from any ideas, methods, instructions or products referred to in the content.